Manuscript Details

Manuscript number	AIIM_2018_391
Title	Recursive Model Identification for the Analysis of the Autonomic Response to Exercise Testing in Brugada Syndrome
Article type	Research Paper

Abstract

This paper proposes the integration and analysis of a closed-loop model of the baroreflex and cardiovascular systems, focused on a time-varying estimation of the autonomic modulation of heart rate in Brugada syndrome (BS), during exercise and subsequent recovery. Patient-specific models of 44 BS patients at different levels of risk (symptomatic and asymptomatic) were identified through a recursive evolutionary algorithm. After parameter identification, a close match between experimental and simulated signals (mean error = 0.81%) was observed. The model-based estimation of vagal and sympathetic contributions were consistent with physiological knowledge, enabling to observe the expected autonomic changes induced by exercise testing. In particular, symptomatic patients presented a significantly higher parasympathetic activity during exercise, and an autonomic imbalance was observed in these patients at peak effort and during post-exercise recovery. A higher vagal modulation during exercise, as well as an increased parasympathetic activity at peak effort and a decreased vagal contribution during post-exercise recovery could be related with symptoms and, thus, with a worse prognosis in BS. This work proposes the first evaluation of the sympathetic and parasympathetic responses to exercise testing in patients suffering from BS, through the recursive identification of computational models; highlighting important trends of clinical relevance that provide new insights into the underlying autonomic mechanisms regulating the cardiovascular system in BS.

Keywords	Autonomic nervous system; Brugada syndrome; computational model; recursive identification
Manuscript region of origin	Europe
Corresponding Author	Mireia Calvo
Order of Authors	Mireia Calvo, Virginie Le Rolle, Daniel Romero, Nathalie Béhar, Pedro Gomis, Philippe Mabo, Alfredo Hernández

Submission Files Included in this PDF

File Name [File Type]

cover_letter1.pdf [Cover Letter]

Highlights.pdf [Highlights]

AIM_exercise.pdf [Manuscript File]

suppl.pdf [Table]

Submission Files Not Included in this PDF

File Name [File Type]

1st_submission_AIM.zip [LaTeX Source File]

To view all the submission files, including those not included in the PDF, click on the manuscript title on your EVISE Homepage, then click 'Download zip file'.

Recursive Model Identification for the Analysis of the Autonomic Response to Exercise Testing in Brugada Syndrome

Mireia Calvo[a], Virginie Le Rolle[a,*], Daniel Romero[b], Nathalie Béhar[a], Pedro Gomis[c,d], Philippe Mabo[a], Alfredo I Hernández[a]

[a] *Univ Rennes, CHU Rennes, Inserm, LTSI UMR 1099, F-35000 Rennes, France.*
[b] *Institute for Bioengineering of Catalonia, Barcelona, E-08930,France*
[c] *Universitat Politécnica de Catalunya, Barcelona, E-08028, Spain*
[d] *CIBER of Bioengineering, Biomaterials and Nanomedicine, Zaragoza, E-50018, Spain*

Abstract

This paper proposes the integration and analysis of a closed-loop model of the baroreflex and cardiovascular systems, focused on a time-varying estimation of the autonomic modulation of heart rate in Brugada syndrome (BS), during exercise and subsequent recovery. Patient-specific models of 44 BS patients at different levels of risk (symptomatic and asymptomatic) were identified through a recursive evolutionary algorithm. After parameter identification, a close match between experimental and simulated signals (mean error = 0.81%) was observed. The model-based estimation of vagal and sympathetic contributions were consistent with physiological knowledge, enabling to observe the expected autonomic changes induced by exercise testing. In particular, symptomatic patients presented a significantly higher parasympathetic activity during exercise, and an autonomic imbalance was observed in these patients at peak effort and during post-exercise recovery. A higher vagal modulation during exercise, as well as an increased parasympathetic activity at peak effort and a decreased vagal contribution during post-exercise recovery could be related with symptoms and, thus, with a worse prognosis in BS. This work proposes the first evaluation of the sympathetic and parasympathetic responses to exercise testing in patients

*Corresponding author (Tel: +33 2 23 23 62 20; Fax: +33 2 23 23 69 17)
Email address: virginie.lerolle@univ-rennes1.fr (Virginie Le Rolle)

suffering from BS, through the recursive identification of computational models; highlighting important trends of clinical relevance that provide new insights into the underlying autonomic mechanisms regulating the cardiovascular system in BS.

Keywords: Autonomic nervous system, Brugada syndrome, computational model, recursive identification

1. Introduction

Brugada syndrome (BS) is an inherited disorder presenting a distinctive electrocardiographic pattern associated with an elevated risk for sudden cardiac death (SCD) [1]. Major cardiac events in this population typically occur at rest and mainly at night, suggesting that the autonomic nervous system (ANS) function, and more specifically the parasympathetic activity, may play a relevant role in the pathophysiology, arrhythmogenesis and prognosis of the disease [2, 3, 4].

However, previous studies on the ANS function of BS patients have led to conflicting results, particularly when based on long-term measurements. Krittayapong et al. concluded that BS patients showed a decreased heart rate variability (HRV) and vagal tone at night compared to controls; as well as a lower diurnal and higher overnight heart rate (HR) when symptomatic patients were compared to asymptomatic subjects and controls [5]. Likewise, Hermida et al. found significantly lower HRV values at night on symptomatic patients [6]; and Pierre et al. observed a decreased HRV in BS patients, with respect to healthy subjects [7]. Results from Tokuyama et al. also showed a significant HRV reduction on BS patients with respect to controls, as well as on both sympathetic and parasympathetic tones and on their circadian variation over 24 hours [8].

In a previous study from our team [9], although symptomatic BS patients showed a decreased heart rate variability and complexity at night, with respect to asymptomatic subjects, no significant differences were observed be-

tween groups on sympathetic and parasympathetic modulations. On the other hand, in Nakazawa et al., results showed higher vagal and reduced sympathetic tones in symptomatic BS patients [10]. Likewise, in a recent work from Behar et al., symptomatic subjects showed an increased parasympathetic activity during both daytime and nighttime, when compared to asymptomatic patients [11]. Finally, HRV analysis in Kostopoulou et al. did not reveal any significant difference between BS patients and controls [12].

Thus, in order to better characterize autonomic modulation, standard maneuvers such as exercise testing can be applied. Exertion causes a sympathetic activation that, together with a parasympathetic inhibition, increases HR, a reliable indicator to evaluate cardiac autonomic function [13]. Conversely, post-exercise cardiodeceleration is adjusted by parasympathetic activation and sympathetic withdrawal [14]. Indeed, some studies have already reported the potential of exercise testing in BS [15, 16, 17, 18]. Amin et al. [19] found a higher parasympathetic reactivation during early recovery after exertion in BS patients with prior ventricular fibrillation events. Likewise, Makimoto et al. concluded that a higher vagal activity after exercise was related to the occurrence of cardiac events in BS [20].

Although classical temporal and spectral markers are widely used in clinical practice for ANS analysis [21], conventional methods have failed to estimate sympathetic and parasympathetic responses to exercise, even in healthy subjects [22], but also in Brugada syndrome patients [18, 23]. Nevertheless, since computational models can directly represent interactions between the cardiovascular system (CVS) and the ANS, model-based reasoning could provide useful knowledge to support autonomic response interpretation in BS. Indeed, in a previous work, we already reported the feasibility of the application of such computational models to reproduce cardiovascular data acquired during head-up tilt testing on a healthy subject and on a BS patient [24]. However, the identification method applied to the system-level models used in this work could only explain the mechanical, circulatory and autonomic sympathetic functions of the cardiovascular system. To tackle this limitation, high-frequency oscillations in-

duced by the parasympathetic regulation of the ANS can be estimated through recursive identification.

Therefore, in this work we propose a novel approach based on the recursive identification of a closed-loop mathematical model of the baroreflex and cardiovascular systems, in order to estimate the time-varying sympathetic and parasympathetic contributions to HR modulation during exercise and subsequent recovery on Brugada patients. Patient-specific models were adjusted for 44 BS patients with different levels of risk (13 symptomatic and 31 asymptomatic) so as to reproduce their HR during exercise testing and, thus, analyze their underlying autonomic function. The paper is organized as follows: in section 2, the experimental protocol and data under study are presented, the computational model is described and the recursive identification method is explained. In section 3, the results of applying the described methods are presented and discussed. Conclusions are finally specified in section 4.

2. Material and Methods

2.1. Study population

The standard 12-lead ECG recordings from 44 patients diagnosed with BS who took part in a physical stress test were collected during a multicentric study conducted in the Cardiology department of the Rennes University Hospital (France). Participants were enrolled in 6 French hospitals located in Rennes, Saint Pierre de la Reunion, Nantes, Bordeaux, Brest and La Rochelle. The study protocol was approved by the respective local ethics committees and all patients provided written informed consent before participation.

In accordance with current guidelines [25], BS was diagnosed when a coved ST-segment elevation (≥ 0.2 mV) was identified in at least one right precordial lead (V1 and/or V2) located in the 2^{nd}, 3^{rd} or 4^{th} intercostal space, in the presence or absence of sodium-channel-blocking agent.

In order to characterize populations with different levels of risk, patients were classified as symptomatic or asymptomatic, based on their medical his-

tory. Thirteen patients presented documented symptoms of ventricular origin: syncope (61.5%), cardiac arrest (38.5%) and dizziness (15.4%), whereas the remaining 31 patients were considered as asymptomatic.

Patients age ranged from 19 to 74 years old (45.07 ± 12.59 years old) and 33 (75%) were males. ICD implantation had been performed in 6 of 31 (19.4%) asymptomatic patients, based on a positive EPS test, whereas all symptomatic patients were ICD carriers. Among 31 patients (11 were symptomatic) in whom genetic screening was performed, an *SCN5A* mutation was found in 13 (41.9%), from whom 6 were symptomatic.

Table 1 summarizes the clinical characteristics of patients included in the study. Since all between-groups differences, apart from ICD implantation, were statistically non-significant, similar baseline characteristics were assumed between populations.

Table 1: Clinical characteristics of BS patients.

	Symptomatic (n=13)	**Asymptomatic (n=31)**	***p*-value**
Age, *years old*	43.62 ± 14.51	45.68 ± 11.90	0.322
Male sex, *n (%)*	11 (84.6%)	22 (71%)	0.355
ICD implantation, *n (%)*	13 (100%)	6 (19.4%)	<0.001
***SCN5A* mutation,** *n (%)*	6 (46.2%)	5 (25%)	0.311

Values are mean ± standard deviation or number of observations (%).
Comparisons are based on Mann-Whitney U non-parametric tests.

2.2. Experimental protocol and data

Participants underwent a triangular exercise test recommended by the American Heart Association [26], which was performed on a cyclo ergometer (Ergoline 900 Egamed, Piestany, Slovakia) and divided in the following phases, represented in Fig. 1:

- Exercise phase:

  - Warm-up phase: for men, initial load of 50 watts (W); for women, initial load of 30 W, both for 2 minutes.
  - Incremental exercise phase: for men, initial load of 80 W for 2 minutes and then incrementing 20 W every 2 minutes; for women, initial load of 50 W, increasing 20 W every 2 minutes. For each patient, the load was increased until it reached the 80% of his/her theoretical maximum heart rate, defined by the formula $MHR = 220 - age$ [27].

- Recovery phase: for men, fixed load of 50 W; for women, fixed load of 30 W, both for 3 minutes.

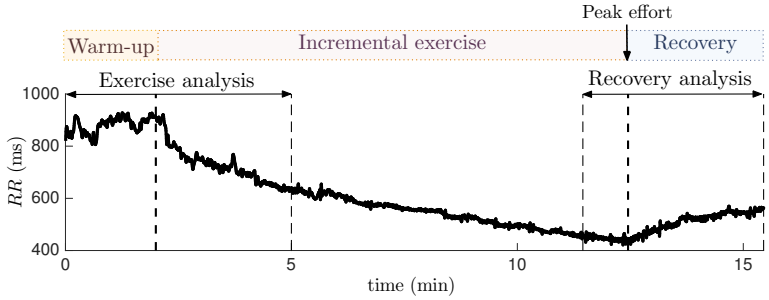

Figure 1: Representative example of RR-interval series observed during the exercise test. The test was divided in three phases: warm-up, incremental exercise and recovery. Due to differences in exercise durations for each patient, recursive identifications were separately performed at the beginning and at the end of the test (exercise and recovery analysis, respectively). Exercise analysis included the warm-up phase and the first 3 minutes of incremental exercise; while recovery analysis was based on the last minute of exertion before peak effort and the recovery phase.

ECG data were acquired with the Holter monitor (ELA medical, Sorin Group, Le Plessis Robinson, France) at a sampling frequency of 1000 Hz. From these signals, RR-interval series were extracted from the lead presenting the highest signal-to-noise ratio (SNR), by means of a noise-robust wavelet-based algorithm for QRS-complex detection and subsequent R-wave peak location [28]. Since the result is a non-uniformly sampled signal, a cubic-spline interpolation was applied to RR-interval time series, to obtain regularly sampled data at a

rate of 10 Hz, which was the sample rate chosen for the model.

2.3. Computational model

Based on our previous works in cardiovascular modeling [29, 30, 31, 24], the proposed model was composed of two coupled submodels representing the cardiovascular system (CVS) and the baroreceptors reflex system (BRS), connected through the HR resulting from the BRS submodel and the systemic arterial pressure coming from the CVS.

2.3.1. Cardiovascular system

As illustrated in Fig. 2, the hemodynamic effects of exercise testing were represented by implementing the cardiovascular model defined in [32].

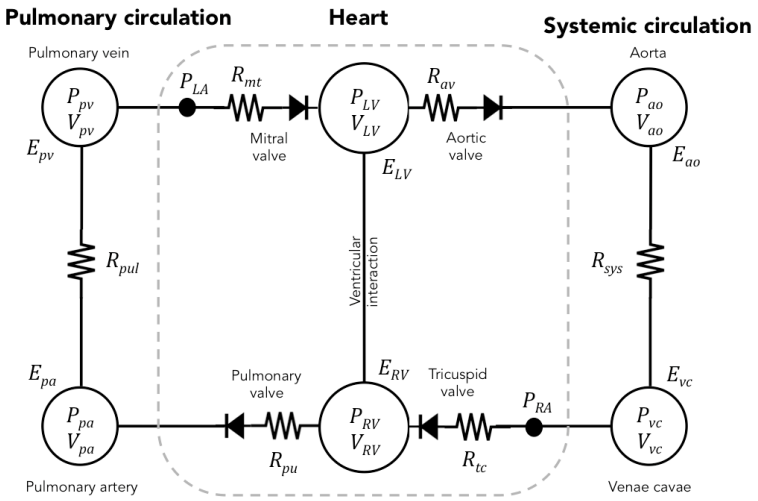

Figure 2: Closed-loop model of the cardiovascular system. E: elastance; R: resistance; P: pressure; V: volume; sys: systemic; pul: pulmonary; pv: pulmonary vein; pa: pulmonary artery; pu: pulmonary valve; av: aortic valve; tc: tricuspid valve; mt: mitral valve; ao: aorta; vc: venae cavae; LA: left atrium; LV: left ventricle; RA: right atrium; RV: right ventricle.

Volumes (V) from each cardiac chamber are obtained from the integral of their respective net flows ($Q_{in} - Q_{out}$). Blood pressure (P) is then computed

from the pressure-volume relationships associated with systole (P_{es}) and diastole (P_{ed}), and a periodic function ($e(t)$) drives the transition between these relationships as follows:

$$P(V,t) = e(t)P_{es}(V) + (1 - e(t))P_{ed}(V)\,, \tag{1}$$

$$P_{es}(V) = E \cdot (V - V_d)\,, \tag{2}$$

$$P_{ed}(V) = P_0 \cdot (\exp[\lambda(V - V_0)] - 1)\,, \tag{3}$$

$$e(t) = A \cdot \exp[-B \cdot ((t - t_s) - C)^2]\,. \tag{4}$$

E refers to the systolic elastance and V_d is the dead volume, respectively representing the slope and intercept of the linear pressure-volume relationship associated with systole. During diastole, this relationship is non-linear and is described by a gradient (P_0), a curvature (λ) and a volume at zero pressure (V_0). Eq. 4 defines the transition between diastolic and systolic dynamics, modulated by a Gaussian function with amplitude A, width B and center C; and t_s refers to the cardiac cycle onset, determined by the HR resulting from the BRS submodel.

Atria were not included in the model since they minimally contribute to main cardiac trends. However, in order to account for relevant ventricular interactions, ventricles were coupled through the septum, represented as a flexible common wall between left and right ventricles. The left ventricle (LV) free wall volume (V_{LVf}) and the right ventricle (RV) free wall volume (V_{RVf}) are defined as:

$$V_{LVf} = V_{LV} - V_{spt}\,, \tag{5}$$

$$V_{RVf} = V_{RV} + V_{spt}\,. \tag{6}$$

where V_{spt}, V_{LV} and V_{RV} are respectively the septum, LV and RV volumes. Then, the septum volume results from linking the septum pressure (P_{spt}) to the difference between left and right ventricular pressures:

$$P_{spt} = P_{LV} - P_{RV}\,, \tag{7}$$

$$P_{spt} = e(t)E_{spt} \cdot (V_{spt} - V_{d,spt}) \tag{8}$$

$$+(1 - e(t))P_{0,spt}(\exp[\lambda(V - V_0)] - 1). \tag{9}$$

Diodes simulate the one-way direction of blood when passing through valves located at the inlet and exit of ventricles. Pressures on the peripheral circulation systems are calculated as a linear relationship between their volume and vascular elastance, following eq. 2. Finally, flows between chambers are obtained from the equation $Q = \frac{\Delta P}{R}$, where ΔP is the pressure gradient between two chambers and R accounts for the corresponding vascular resistance connecting them.

2.3.2. Baroreflex model

Sympathetic and parasympathetic efferent responses to arterial blood pressure regulation were modeled based on a widely used approach [33, 34], represented in Fig. 3.

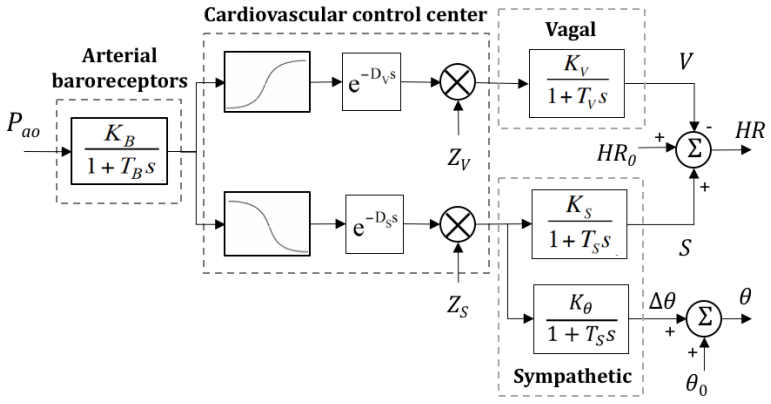

Figure 3: Diagram of the baroreflex model for cardiovascular regulation. From the arterial pressure registered at the systemic circulation (P_{ao}), the baroreflex system controls heart rate (HR) and other cardiovascular variables (θ), such as ventricular contractility or elastance, systemic resistance and venous dead volume.

The systemic arterial pressure registered at the CVS submodel was used as

the input pressure for the baroreflex system which, in turn, modulated the HR used as input of the CVS submodel, thus defining the closed-loop model.

Baroreceptors dynamical properties are represented by a first-order transfer function, whose gain and time constant are K_B and T_B. Then, cardiovascular control is represented, in both sympathetic and vagal branches, by a sigmoidal function and delays D_S and D_V, respectively. Sympathetic and parasympathetic contributions are modulated by two time-varying variables, Z_S and Z_V, to account for the influence of exogenous phenomena and collect all the variability caused by sources other than blood pressure fluctuations (central modulation, respiration, etc.).

For chronotropic regulation, each efferent pathway is finally modeled with a first-order filter, characterized by a gain (K_V, K_S) and a time constant (T_V, T_S). The output HR is the result of adding the contributions of both sympathetic (S) and vagal (V) branches to the intrinsic heart rate (HR_0):

$$HR = HR_0 + S - V. \tag{10}$$

Finally, other sympathetic branches control ventricular contractility (E), systemic resistance (R) and venous dead volume (VV) through a first-order filter characterized by the sympathetic time constant T_S and the gain related to each branch K_θ, where $\theta \in \{E, R, VV\}$. Being θ_0 the baseline response and $\Delta\theta$ the baroreflex regulation, the output response for each regulated variable is defined as:

$$\theta = \theta_0 + \Delta\theta. \tag{11}$$

2.4. Recursive identification

All model parameters other than Z_S and Z_V were fixed based on the literature [32, 33, 35]. Their values are provided as Supplementary material (Tables I and II).

As illustrated in Fig. 4, at each step i of the recursive algorithm, parameters Z_S and Z_V were identified on a time interval T_I of duration largely inferior to

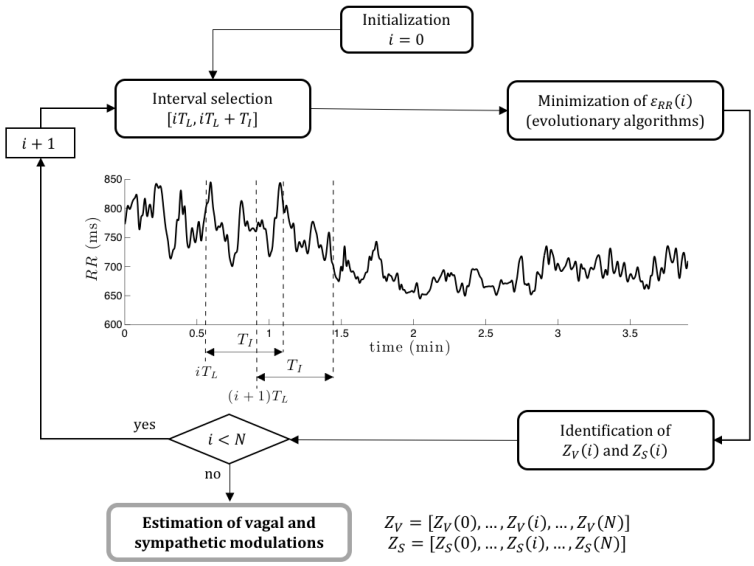

Figure 4: Diagram of the recursive identification algorithm and time windows involved. T_L: overlap window; T_I: identification window; ϵ_{RR}: error function. For visualization purposes, T_L and T_I temporal supports were enlarged in this figure and do not illustrate representative time windows.

the RR-interval series length ($T_I << T_{TOT}$). At each step, simulated and experimental signals were compared in order to minimize the error function $\epsilon_{RR}(i)$, defined as:

$$\epsilon_{RR}(i) = \sum_{t_e=iT_L}^{(i+1)T_L} |RR_{sim}(t_e) - RR_{exp}(t_e)| \; + \sum_{t_e=iT_L}^{iT_L+T_I} |RR_{sim}(t_e) - RR_{exp}(t_e)|, \quad i \in [0, \cdots, N] \quad (12)$$

where t_e is the time elapsed since the onset of the identification period, T_L corresponds to the overlap time between each interval and $N = \lfloor T_{TOT}/T_L \rfloor$ is the number of identification intervals. The time windows involved in the recursive identification algorithm are also represented in Fig. 4.

The overlap time duration T_L was set equal to the parasympathetic time

constant (T_V) to capture rapid fluctuations due to vagal response; whereas interval T_I was set as the sympathetic time constant (T_S) in order to take into account the low frequency component causing RR-interval series slow variations.

As in previous works of our team [36, 37], the best set of $\{Z_S,\ Z_V\}$ parameters for each patient was identified on each interval i, through an approach based on evolutionary algorithms [38]. The initial population, or first set of candidate optimization solutions, was randomly generated. For the following steps, assuming limited parameter variations between intervals, the initial population was set equal to that obtained from the previous interval $i-1$. Although this approach limits parameter variations, mutation probability was set to $p_m = 0.2$ in order to stimulate the exploration of the entire search space and prevent from convergence to local minima.

These recursive identifications were separately performed during exercise and recovery. Since each patient test differed in the incremental exercise phase duration and the shortest case in our clinical series lasted less than 5 minutes, as represented in Fig. 1, for exercise analysis, only the warm-up phase and the first 3 minutes of incremental exertion were identified. Then, for recovery analysis, the last minute of exertion and the first 3 minutes of recovery, were assessed.

In order to quantify identification performance, the error between simulated and experimental RR-interval series for both exercise ($E_{exercise}$) and recovery ($E_{recovery}$) phases was expressed in percentage and computed as:

$$E = \frac{1}{n}\sum_{i=1}^{n} |100 \cdot \frac{RR_{sim}(i) - RR_{exp}(i)}{RR_{exp}(i)}|, \tag{13}$$

where n is the number of samples being compared. Due to identification errors caused by initialization, the first minute of warm-up was removed from exercise analysis, as well as the first 30 seconds of the last minute of exertion were eliminated from recovery analysis.

2.5. Statistical analysis

The identified time-varying sympathetic (S) and parasympathetic (V) contributions to exercise and subsequent recovery were then compared between

symptomatic and asymptomatic patients, by Mann-Whitney U non-parametric tests. In order to compare the last minute of exertion and recovery, all patients were synchronized with respect to the peak effort instant.

The autonomic response to exercise testing was also analyzed by fitting linear regression models to the estimated S and V of each patient, for the last minute of warm-up, the first, second and third minutes of incremental exercise, the last 30 seconds of exertion, and the first, second and third minutes of recovery.

3. Results and Discussion

Based on visual inspection and error results ($E_{exercise} = 1.10 \pm 0.54\%$, $E_{recovery} = 0.52 \pm 0.16\%$), a satisfactory agreement was observed between simulated signals and real data, leading to errors always inferior to 3.5%. Fig. 5 illustrates an example of simulated and experimental RR-interval series during the last minute of warm-up and the first 3 minutes of incremental exercise ($E = 1.7\%$).

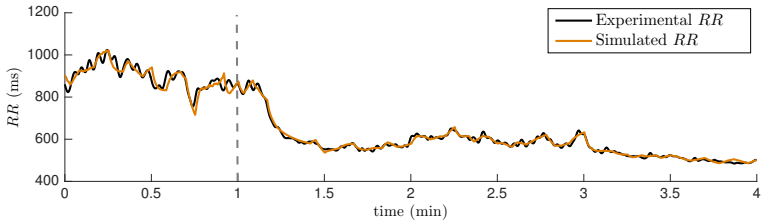

Figure 5: Simulated (orange) and experimental (black) RR-interval series during the last minute of warm-up and the first 3 minutes of incremental exercise. $E = 1.7\%$. The dashed vertical line delimits the end of warm-up and subsequent incremental exercise onset.

Fig. 6 shows the mean vagal and sympathetic contributions of the autonomic response to exertion, for symptomatic and asymptomatic patients. In both groups, vagal modulation remained low along the whole exercise phase and decreased as the test progressed. Conversely, sympathetic contribution increased during exercise, and specially after warm-up. Moreover, symptomatic patients presented significantly higher parasympathetic values around the sec-

ond minute of incremental exercise, and mainly at the end of warm-up, where this group also presented significantly higher sympathetic values.

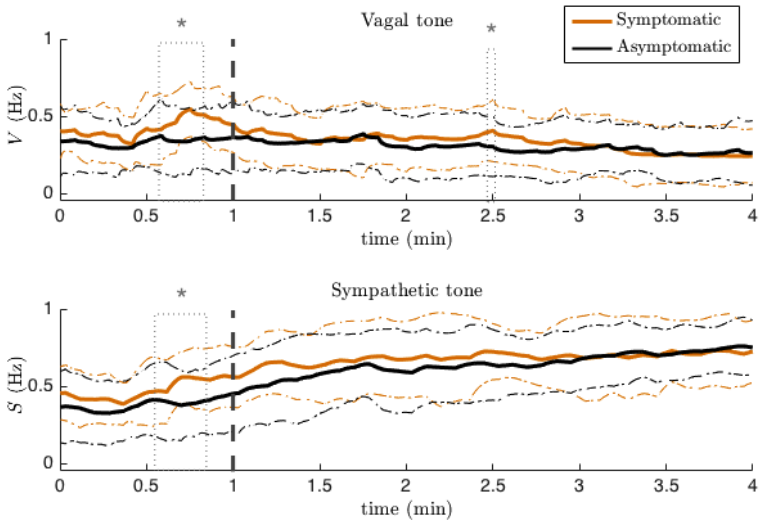

Figure 6: Mean estimation of vagal (V) and sympathetic (S) contributions, for symptomatic (orange) and asymptomatic (black) patients, during exercise. Dashed vertical lines delimit the end of warm-up and subsequent incremental exercise onset. Pointed boxes indicate those segments where significant differences between groups ($^*p < 0.05$) were found. Dashed horizontal lines represent the standard deviations for each group.

These results are in agreement with those found in the literature, where a higher vagal modulation has been observed in symptomatic BS patients [11, 10]. Although some significant differences were also found after 1 minute of incremental exercise, the largest and most significant segment was observed at the end of warm-up. Moreover, sympathetic activity in this phase was also found to be higher in symptomatic patients, contrary to tendencies found in previous publications based on classical spectral markers [8, 10]. Nevertheless, many studies on cardiac autonomic function based on classic approaches have failed to represent the sympathetic response to exercise testing, even in healthy subjects [22], since the LF component does not provide an index of sympathetic tone but rather reflects a complex interplay among many factors including the sympathetic and parasympathetic contributions to ANS. Similarly, our previous works

based on conventional time-frequency methods failed to estimate the autonomic response to exercise testing in this population [18, 23]. Thus, model-based reasoning may provide better estimations of the sympathetic and parasympathetic contributions to HR modulation during exercise.

In Fig. 7, the mean vagal and sympathetic contributions during recovery, for symptomatic and asymptomatic patients, are represented. After the peak effort, an increase in parasympathetic activity, as well as a decrease in sympathetic modulation can be observed for both groups. Although no statistically significant differences related to symptomatic status were found on the vagal modulation, at the end of the second minute of recovery, symptomatic patients presented significantly lower sympathetic values. These findings concur with a previous work where a lower sympathetic activity was reported in symptomatic patients [10].

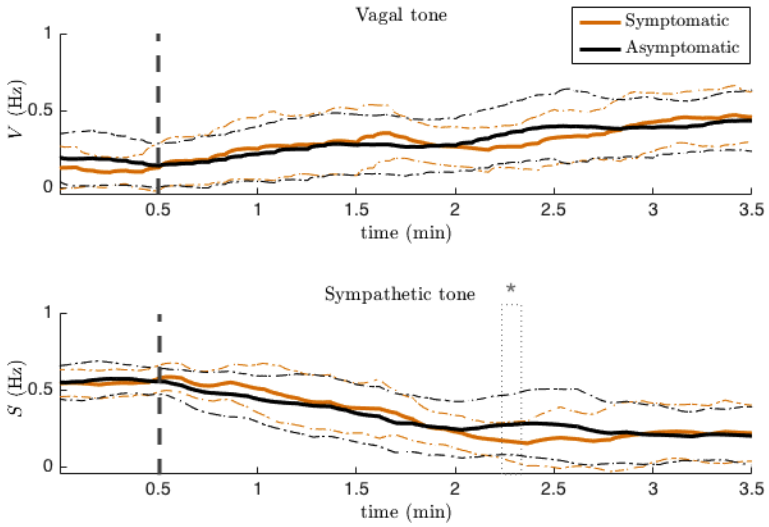

Figure 7: Mean estimation of vagal (V) and sympathetic (S) contributions, for symptomatic (orange) and asymptomatic (black) patients, during post-exercise recovery. Dashed vertical lines delimit the end of exertion and subsequent recovery onset. The pointed box indicates the segment where significant differences between groups ($^*p < 0.05$) were found. Dashed horizontal lines represent the standard deviations for each group.

Finally, the slopes from the adjusted linear regression models were compared

between symptomatic and asymptomatic populations. Since no statistically significant results were obtained during exercise analysis, Table 2 summarizes, for each analyzed period during recovery, the mean ± standard deviation values obtained for each group of patients, together with their associated p-values.

Table 2: Mean ± standard deviation slopes for sympathetic and parasympathetic contributions (in Hz), and associated p-values, from symptomatic and asymptomatic patients, at peak effort and during different periods of recovery after exertion (*p <0.05). Comparisons are based on Mann-Whitney U non-parametric tests.

	Symptomatic (n=13)	**Asymptomatic (n=31)**	p**-val**
Peak effort (30 sec)			
Sympathetic	0.09 ± 0.30	-0.03 ± 0.25	0.26
Parasympathetic	**0.09 ± 0.22**	**-0.11 ± 0.25**	**0.03***
Recovery (1^{st} min)			
Sympathetic	-0.21 ± 0.26	-0.18 ± 0.27	0.72
Parasympathetic	0.15 ± 0.29	0.15 ± 0.25	0.82
Recovery (2^{nd} min)			
Sympathetic	-0.22 ± 0.22	-0.02 ± 0.35	0.05
Parasympathetic	**-0.03 ± 0.18**	**0.16 ± 0.33**	**0.04***
Recovery (3^{rd} min)			
Sympathetic	0.13 ± 0.40	-0.11 ± 0.51	0.12
Parasympathetic	0.26 ± 0.46	-0.01 ± 0.51	0.11

Symptomatic and asymptomatic patients showed significant differences in vagal modulation, when compared at peak effort and during the second minute of recovery. Fig. 8 illustrates the mean slope for symptomatic and asymptomatic populations at peak effort and during recovery, highlighting those segments where significant differences were found.

Although results show non-negligible standard deviations, on average, the simulated vagal contribution was consistent with physiological knowledge on asymptomatic patients, decreasing at peak effort and increasing during post-

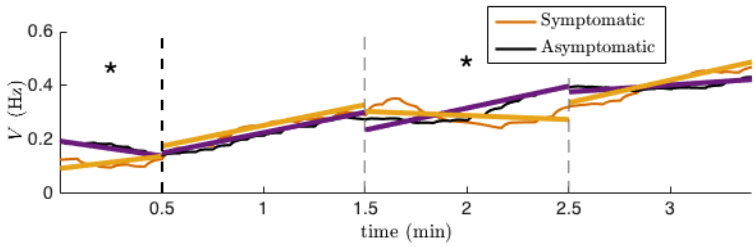

Figure 8: Mean linear regression models adjusted to the estimation of vagal modulation at peak effort and during post-exercise recovery, for symptomatic (orange) and asymptomatic (black) patients. Dashed vertical lines delimit the analyzed periods and segments presenting statistically significant differences between populations are noted ($^*p < 0.05$).

exercise recovery. However, significant alterations were noted on symptomatic patients, showing a mean positive slope at peak effort and a descending trend during the second minute of recovery.

Thus, these findings provide further evidence for the role of autonomic imbalance in the pathophysiology of BS. However, since this study is based on a relatively small population of 44 BS patients, the moderately significant differences found between analyzed groups should be interpreted carefully. Indeed, the fact that corrected p-values would lead to non-significant results, indicates that reliable physiological interpretations should be extracted by means of larger clinical series. Moreover, the analyzed population presents a significant imbalance between symptomatic and asymptomatic groups; although this is a common scenario in BS, where symptoms refer to recovered SCD or syncope and, thus, they are usually found in a small amount of patients. Likewise, most previously reported studies on BS autonomic function are based on clinical series of similar, or even smaller, sizes [5, 6, 10, 7, 12, 8], as well as most works reporting the identification of computational models are based on small populations.

Thus, the implemented model-based approach provides the first time-varying autonomic estimation in the context of BS, highlighting the relevance of exercise testing in order to unmask significant changes in ANS modulation that may not be captured at daytime, during a regular ECG examination. Indeed, this

altered autonomic cardiac system dynamics during post-exercise recovery, when vagal contribution is predominant, concurs with previous studies reporting an increase in Brugada-like ECG changes induced during vagal stimulation [39], as well as with the fact that most life-threatening cardiac arrhythmias in BS occur at rest and during sleep, when parasympathetic activity is predominant [40, 2]. Furthermore, the results confirm previous findings where symptomatic BS patients showed a higher vagal modulation [11, 10, 8] with respect to asymptomatic patients, supporting the idea that increased vagal responses could be related to a worse prognosis in Brugada syndrome.

4. Conclusions

Conventional methods have been proved insufficient for autonomic function analysis. Therefore, in this work, we propose an original model-based approach to characterize ANS dynamics in response to exertion. It is based on a recursively identified closed-loop model of the baroreflex and cardiovascular systems, introducing: i) patient-specific model parameter recursive identifications and ii) estimations of the time-varying sympathetic and parasympathetic modulations of the heart rate.

The model was evaluated with data from 44 BS patients, acquired during exercise testing, to compare the autonomic function of symptomatic and asymptomatic BS populations. Results show a close match between experimental and simulated signals. Moreover, estimations of sympathetic and parasympathetic components were consistent with physiological knowledge, showing the feasibility of the model to reproduce realistic autonomic responses to exercise.

According to results, a significantly higher parasympathetic activity was observed in symptomatic patients during exercise, providing further evidence for the role of vagal contribution in BS prognosis. Moreover, during post-exercise recovery, parasympathetic modulation on symptomatic patients indicated an autonomic imbalance. Thus, this original approach enables to unmask indicators capturing cardiovascular and autonomic dynamics, never before studied in

BS, that may be useful for risk stratification. Indeed, we believe that a robust BS risk stratification should be based on a combination of both classical electrophysiological features, but also on this kind of markers providing an improved estimation of the autonomic activity.

More extensive evaluations including a wider range of parameters, a greater population of patients, as well as the possibility of adjusting parameters based on not only the HR, but also the blood pressure, should be performed in the future. Furthermore, the proposed model could be enriched by including a representation of cardiorespiratory interactions [33].

Nevertheless, this paper presents the first model-based approach towards the evaluation of the time-varying autonomic response to exertion in BS patients, showing results that indicate trends of clinical relevance and, thus, provide a step forward towards the understanding of the disease.

5. Acknowledgements

This work was supported by the French Ministry of Health (Programme Hospitalier de Recherche Clinique - PHRC Regional). M. Calvo thanks la Caixa Foundation and D. Romero acknowledges Lefoulon-Delalande Foundation for financial support.

References

[1] P. Brugada, J. Brugada, Right bundle branch block, persistent st segment elevation and sudden cardiac death: a distinct clinical and electrocardiographic syndrome: a multicenter report, Journal of the American College of Cardiology 20 (6) (1992) 1391–1396.

[2] K. Matsuo, T. Kurita, M. Inagaki, M. Kakishita, N. Aihara, W. Shimizu, A. Taguchi, K. Suyama, S. Kamakura, K. Shimomura, The circadian pattern of the development of ventricular fibrillation in patients with brugada syndrome, European heart journal 20 (6) (1999) 465–470.

[3] G.-X. Yan, C. Antzelevitch, Cellular basis for the brugada syndrome and other mechanisms of arrhythmogenesis associated with st-segment elevation, Circulation 100 (15) (1999) 1660–1666.

[4] K. Mizumaki, A. Fujiki, T. Tsuneda, M. Sakabe, K. Nishida, M. Sugao, H. Inoue, Vagal activity modulates spontaneous augmentation of st elevation in the daily life of patients with brugada syndrome, Journal of cardiovascular electrophysiology 15 (6) (2004) 667–673.

[5] R. Krittayaphong, G. Veerakul, K. Nademanee, C. Kangkagate, Heart rate variability in patients with brugada syndrome in thailand, European Heart Journal 24 (19) (2003) 1771–1778.

[6] J.-S. Hermida, A. Leenhardt, B. Cauchemez, I. Denjoy, G. Jarry, F. Mizon, P. Milliez, J.-L. Rey, P. Beaufils, P. Coumel, Decreased nocturnal standard deviation of averaged nn intervals, European heart journal 24 (22) (2003) 2061–2069.

[7] B. Pierre, D. Babuty, P. Poret, C. Giraudeau, O. Marie, P. Cosnay, L. Fauchier, Abnormal nocturnal heart rate variability and qt dynamics in patients with brugada syndrome, Pacing and clinical electrophysiology 30 (s1) (2007) S188–S191.

[8] T. Tokuyama, Y. Nakano, A. Awazu, Y. Uchimura-Makita, M. Fujiwra, Y. Watanabe, A. Sairaku, K. Kajihara, C. Motoda, N. Oda, et al., Deterioration of the circadian variation of heart rate variability in brugada syndrome may contribute to the pathogenesis of ventricular fibrillation, Journal of cardiology 64 (2) (2014) 133–138.

[9] M. Calvo, V. Le Rolle, D. Romero, N. Béhar, P. Gomis, P. Mabo, A. Hernández, Heart rate differences between symptomatic and asymptomatic brugada syndrome patients at night, Physiological measurement 39 (6) (2018) 065002.

[10] K. Nakazawa, T. Sakurai, A. Takagi, R. Kishi, K. Osada, T. Nanke, F. Miyake, N. Matsumoto, S. Kobayashi, Autonomic imbalance as a property of symptomatic brugada syndrome, Circulation journal 67 (6) (2003) 511–514.

[11] N. Behar, B. Petit, V. Probst, F. Sacher, G. Kervio, J. Mansourati, P. Bru, A. Hernandez, P. Mabo, Heart rate variability and repolarization characteristics in symptomatic and asymptomatic brugada syndrome, Europace 19 (10) (2017) 1730–1736. doi:10.1093/europace/euw224.

[12] A. Kostopoulou, M. Koutelou, G. Theodorakis, A. Theodorakos, E. Livanis, T. Maounis, A. Chaidaroglou, D. Degiannis, V. Voudris, D. Kremastinos, et al., Disorders of the autonomic nervous system in patients with brugada syndrome: a pilot study, Journal of cardiovascular electrophysiology 21 (7) (2010) 773–780.

[13] M. K. Lahiri, P. J. Kannankeril, J. J. Goldberger, Assessment of autonomic function in cardiovascular disease, Journal of the American College of Cardiology 51 (18) (2008) 1725–1733.

[14] Y. Arai, J. P. Saul, P. Albrecht, L. H. Hartley, L. S. Lilly, R. J. Cohen, W. S. Colucci, Modulation of cardiac autonomic activity during and immediately after exercise, American Journal of Physiology-Heart and Circulatory Physiology 256 (1) (1989) H132–H141.

[15] S. Masrur, S. Memon, P. D. Thompson, Brugada syndrome, exercise, and exercise testing, Clinical cardiology 38 (5) (2015) 323–326.

[16] M. Subramanian, M. A. Prabhu, M. S. Harikrishnan, S. S. Shekhar, P. G. Pai, K. Natarajan, The utility of exercise testing in risk stratification of asymptomatic patients with type 1 brugada pattern, Journal of Cardiovascular Electrophysiology 28 (2017) 677–683.

[17] M. Calvo, P. Gomis, D. Romero, V. Le Rolle, N. Béhar, P. Mabo,

A. Hernández, Heart rate complexity analysis in brugada syndrome during physical stress testing, Physiological measurement 38 (2) (2017) 387–396.

[18] M. Calvo, D. Romero, V. Le Rolle, P. Gomis, N. Behar, P. Mabo, A. Hernandez, Multivariate classification of brugada syndrome patients based on autonomic response to exercise testing, PLoS ONE 13 (5) (2018) e0197367.

[19] A. S. Amin, E. A. de Groot, J. M. Ruijter, A. A. Wilde, H. L. Tan, Exercise-induced ecg changes in brugada syndrome, Circulation: Arrhythmia and Electrophysiology 2 (5) (2009) 531–539.

[20] H. Makimoto, E. Nakagawa, H. Takaki, Y. Yamada, H. Okamura, T. Noda, K. Satomi, K. Suyama, N. Aihara, T. Kurita, et al., Augmented st-segment elevation during recovery from exercise predicts cardiac events in patients with brugada syndrome, Journal of the American College of Cardiology 56 (19) (2010) 1576–1584.

[21] T. F. of the European Society of Cardiology, et al., Heart rate variability standards of measurement, physiological interpretation, and clinical use, European Heart Journal 17 (354–381).

[22] S. Michael, K. S. Graham, G. M. Davis, Cardiac autonomic responses during exercise and post-exercise recovery using heart rate variability and systolic time intervals—a review, Frontiers in Physiology 8 (2017) 301.

[23] M. Calvo, V. Le Rolle, D. Romero, N. Béhar, P. Gomis, P. Mabo, A. Hernández, Sex-specific analysis of the cardiovascular function, 1st Edition, Springer International Publishing, 2018, Ch. 7b: Gender differences in the autonomic response to exercise testing in Brugada syndrome.

[24] M. Calvo, V. Le Rolle, D. Romero, N. Behar, P. Gomis, P. Mabo, A. I. Hernandez, Analysis of a cardiovascular model for the study of the autonomic response of brugada syndrome patients, in: Engineering in Medicine and Biology Society (EMBC), 2016 IEEE 38th Annual International Conference of the IEEE, 2016, pp. 5591–5594.

[25] S. G. Priori, C. Blomström-Lundqvist, A. Mazzanti, N. Blom, M. Borggrefe, J. Camm, P. Elliott, D. Fitzsimons, R. Hatala, G. Hindricks, et al., Task force for the management of patients with ventricular arrhythmias and the prevention of sudden cardiac death of the european society of cardiology (esc). 2015 esc guidelines for the management of patients with ventricular arrhythmias and the prevention of sudden cardiac death: the task force for the management of patients with ventricular arrhythmias and the prevention of sudden cardiac death of the european society of cardiology (esc) endorsed by: Association for european paediatric and congenital cardiology (aepc), Europace 17 (2015) 1601–1687.

[26] R. J. Gibbons, G. J. Balady, J. T. Bricker, B. R. Chaitman, G. F. Fletcher, V. F. Froelicher, D. B. Mark, B. D. McCallister, A. N. Mooss, M. G. O'Reilly, et al., Acc/aha 2002 guideline update for exercise testing: summary article: a report of the american college of cardiology/american heart association task force on practice guidelines (committee to update the 1997 exercise testing guidelines), Journal of the American College of Cardiology 40 (8) (2002) 1531–1540.

[27] S. Fox 3rd, W. Haskell, Physical activity and the prevention of coronary heart disease, Bulletin of the New York Academy of Medicine 44 (8) (1968) 950–965.

[28] J. Dumont, A. I. Hernandez, G. Carrault, Improving ecg beats delineation with an evolutionary optimization process, IEEE Transactions on Biomedical Engineering 57 (3) (2010) 607–615.

[29] A. I. Hernandez, V. Le Rolle, D. Ojeda, P. Baconnier, J. Fontecave-Jallon, F. Guillaud, T. Grosse, R. G. Moss, P. Hannaert, S. R. Thomas, Integration of detailed modules in a core model of body fluid homeostasis and blood pressure regulation, Progress in Biophysics and Molecular Biology 107 (1) (2011) 169–182.

[30] V. Le Rolle, D. Ojeda, A. I. Hernández, Embedding a cardiac pulsatile

model into an integrated model of the cardiovascular regulation for heart failure followup, IEEE transactions on biomedical engineering 58 (10) (2011) 2982–2986.

[31] H. M. Romero-Ugalde, D. Ojeda, V. L. Rolle, D. Andreu, D. Guiraud, J.-L. Bonnet, C. Henry, N. Karam, A. Hagege, P. Mabo, G. Carrault, A. I. Hernandez, Model-based design and experimental validation of control modules for neuromodulation devices, Biomedical Engineering, IEEE Transactions on 63 (7) (2015) 1551–1558.

[32] B. W. Smith, J. G. Chase, R. I. Nokes, G. M. Shaw, G. Wake, Minimal haemodynamic system model including ventricular interaction and valve dynamics, Medical engineering & physics 26 (2) (2004) 131–139.

[33] V. Le Rolle, A. I. Hernández, P.-Y. Richard, G. Carrault, An autonomic nervous system model applied to the analysis of orthostatic tests, Modelling and Simulation in Engineering 2008 (2008) 2.

[34] M. Ursino, E. Magosso, Acute cardiovascular response to isocapnic hypoxia. i. a mathematical model, American Journal of Physiology-Heart and Circulatory Physiology 279 (1) (2000) H149–4165.

[35] A. I. Hernandez Rodriguez, Fusion de signaux et de modèles pour la caractérisation d'arythmies cardiaques, Ph.D. thesis, Université Rennes 1 (2000).

[36] V. Le Rolle, A. Beuchee, J.-P. Praud, N. Samson, P. Pladys, A. I. Hernández, Recursive identification of an arterial baroreflex model for the evaluation of cardiovascular autonomic modulation, Computers in biology and medicine 66 (287–294).

[37] D. Ojeda, V. Le Rolle, M. Harmouche, A. Drochon, H. Corbineau, J.-P. Verhoye, A. I. Hernandez, Sensitivity analysis and parameter estimation of a coronary circulation model for triple-vessel disease, IEEE Transactions on Biomedical Engineering 61 (4) (2014) 1208–1219.

[38] D. E. Goldberg, J. H. Holland, Genetic algorithms and machine learning, Machine learning 3 (2) (1988) 95–99.

[39] T. Ikeda, M. Takami, K. Sugi, Y. Mizusawa, H. Sakurada, H. Yoshino, Noninvasive risk stratification of subjects with a brugada-type electrocardiogram and no history of cardiac arrest, Annals of Noninvasive Electrocardiology 10 (4) (2005) 396–403.

[40] P. Kies, T. Wichter, M. Schäfers, M. Paul, K. P. Schäfers, L. Eckardt, L. Stegger, E. Schulze-Bahr, O. Rimoldi, G. Breithardt, et al., Abnormal myocardial presynaptic norepinephrine recycling in patients with brugada syndrome, Circulation 110 (19) (2004) 3017–3022.

TABLE I
CVS SUBMODEL PARAMETER VALUES.

Parameter	Description	Nominal value
E_{ao}	Aorta elastance (mmHg ml^{-1})	0.705
E_{vc}	Venae cavae elastance (mmHg ml^{-1})	0.011
E_{pa}	Pulmonary artery elastance (mmHg ml^{-1})	0.338
E_{pv}	Pulmonary vein elastance (mmHg ml^{-1})	0.006
E_{LVf}	Left ventricle free wall elastance (mmHg ml^{-1})	3.405
E_{RVf}	Right ventricle free wall elastance (mmHg ml^{-1})	0.653
E_{spt}	Septum elastance (mmHg ml^{-1})	48.754
$V_{d,ao}$	Aorta dead volume (ml)	800
$V_{d,vc}$	Venae cavae dead volume (ml)	2830
$V_{d,pa}$	Pulmonary artery dead volume (ml)	160
$V_{d,pv}$	Pulmonary vein dead volume (ml)	200
$V_{d,LVf}$	Left ventricle free wall dead volume (ml)	5
$V_{d,RVf}$	Right ventricle free wall dead volume (ml)	5
$V_{d,spt}$	Septum dead volume (ml)	2
$V_{0,pcd}$	Pericardium end-diastolic volume (ml)	200
$V_{0,LVf}$	Left ventricle free wall end-diastolic volume (ml)	5
$V_{0,RVf}$	Right ventricle free wall end-diastolic volume (ml)	5
$V_{0,spt}$	Septum elastance end-diastolic volume (ml)	2
λ_{pcd}	Pericardium end-diastolic exponent (ml^{-1})	0.030
λ_{LVf}	Left ventricle free wall end-diastolic exponent (ml^{-1})	0.015
λ_{RVf}	Right ventricle free wall end-diastolic exponent (ml^{-1})	0.015
λ_{spt}	Septum end-diastolic exponent (ml^{-1})	0.435
$P_{0,pcd}$	Intrinsic pericardium pressure (mmHg)	0.500
$P_{0,LVf}$	Intrinsic left ventricle free wall pressure (mmHg)	1.275
$P_{0,RVf}$	Intrinsic right ventricle free wall pressure (mmHg)	1.200
$P_{0,spt}$	Instrinsic septum pressure (mmHg)	1.110
A	Amplitude of Gaussian transition function (n.u.)	1
B	Width of Gaussian transition function (n.u.)	80
C	Center of Gaussian transition function (n.u.)	0.4
R_{mt}	Mitral valve resistance (mmHg s ml^{-1})	0.001
R_{av}	Aortic valve resistance (mmHg s ml^{-1})	0.011
R_{tc}	Tricuspid valve resistance (mmHg s ml^{-1})	0.001
R_{pu}	Pulmonary valve resistance (mmHg s ml^{-1})	0.004
R_{pul}	Pulmonary circularion resistance (mmHg s ml^{-1})	0.143
R_{sys}	Systemic circulation resistance (mmHg s ml^{-1})	1.050
V_{tot}	Total blood volume (ml)	5500
P_{pt}	Thoracic cavity pressure (mmHg)	-4

TABLE II
BRS SUBMODEL PARAMETER VALUES.

Parameter	Description	Nominal value
$HR0$	Intrinsic heart rate (Hz)	1.33
K_B	Baroreceptors gain (n.u.)	1
T_B	Baroreceptors time constant (s)	2
K_V	Gain for vagal heart rate modulation (n.u.)	1
T_V	Vagal time constant (s)	1.5
a_V	Normalization offset for vagal heart rate modulation (n.u.)	0
b_V	Normalization gain for vagal heart rate modulation (n.u.)	1
M_V	Normalization center for vagal heart rate modulation (n.u.)	100
λ_V	Normalization exponent for vagal heart rate modulation (n.u.)	-0.04
D_V	Vagal delay (s)	0.2
K_S	Gain for sympathetic heart rate modulation (n.u.)	1
T_S	Sympathetic time constant (s)	8
a_S	Normalization offset for sympathetic heart rate modulation (n.u.)	0
b_S	Normalization gain for sympathetic heart rate modulation (n.u.)	1
M_S	Normalization center for sympathetic heart rate modulation (n.u.)	100
λ_S	Normalization exponent for sympathetic heart rate modulation (n.u.)	0.09
D_S	Sympathetic delay (s)	2
K_R	Gain for peripheral resistance modulation (n.u.)	1
T_R	Peripheral resistance time constant (s)	8
a_R	Normalization offset for peripheral resistance modulation (n.u.)	0
b_R	Normalization gain for peripheral resistance modulation (n.u.)	1
M_R	Normalization center for peripheral resistance modulation (n.u.)	100
λ_R	Normalization exponent for peripheral resistance modulation (n.u.)	0.09
D_R	Peripheral resistance delay (s)	2
K_{VV}	Gain for venous volume modulation (n.u.)	1
T_{VV}	Venous volume time constant (s)	8
a_{VV}	Normalization offset for venous volume modulation (n.u.)	0
b_{VV}	Normalization gain for venous volume modulation(n.u.)	1
M_{VV}	Normalization center for venous volume modulation (n.u.)	100
λ_{VV}	Normalization exponent for venous volume modulation (n.u.)	0.09
D_{VV}	Venous volume delay (s)	2
K_E	Gain for contractility/elastance modulation (n.u.)	1
T_E	Contractility time constant (s)	8
a_E	Normalization offset for contractility modulation (n.u.)	0
b_E	Normalization gain for contractility modulation (n.u.)	1
M_E	Normalization center for contractility modulation (n.u.)	100
λ_E	Normalization exponent for contractility modulation (n.u.)	0.09
D_E	Contractility delay (s)	2